CREATION OF DATABASE OF EARTHQUAKE RECORDS FROM A REINFORCED CONCRETE TOWER AND OBSERVATION OF SOIL-STRUCTURE INTERACTION EFFECTS

by

Todor Ganev[1], Shigeru Nagata[2] and Tsuneo Katayama[3]

INTRODUCTION

For observation of soil-structure interaction during earthquakes, a reinforced concrete tower is constructed in the Chiba experimental station of the Institute of Industrial Science, University of Tokyo.[1)-5)] The accelerometers, installed in it, are in operation since August 1983 and have provided records from more than 200 earthquakes. The tower is located near the Chiba seismometer array, the records of which are used for the creation of the Chiba array database.[7)] Using the records from the tower accelerometers and some of the accelerometers, which are part of the Chiba array as well, a database of the observation tower response during different earthquakes is created. Experiments with microtremor equipment are made for investigating the small amplitude vibrations of the soil-structure system. Results from processing of microtremor data are compared with results from processing real earthquake data to make conclusions about the influence of the magnitude of the dynamic load on the interaction between soil and structure.

DESCRIPTION OF THE OBSERVATION TOWER AND SURROUNDING SITE CONDITIONS

The observation tower, which has an octagonal cross-section, consists of four floors and a basement, with a total height of 10 m above the ground level and 2.5 m underground shown on Figure 1.[1),2)] The thickness of the walls is 180 mm and the thickness of all slabs is 150 mm, with the exception of the basement floor slab, which

1) Graduate student, Civil Engineering Department, University of Tokyo.
2) Lecturer, Institute of Industrial Science, University of Tokyo.
3) Professor, Institute of Industrial Science, University of Tokyo.

is 500 mm. The floor slab of the second floor has an octagonal opening in the middle. A total of 13 accelerometers is attached to the floor slabs, including the basement floor (Fig.2). Borehole P5 of the Chiba array is located at an approximate distance of 15 m from the tower. The soil profile at it is relatively simple with rather uniform layering (Fig.3)[7]. The top 3-5 m of the site is loam, having standard penetration values N less than 10. Under this layer, there is a diluvium sand layer with N values over 20. Its stiffness increases with the depth, but it is interspersed with clayey layers, which have smaller N values, at certain places below 20. The groundwater table is deeper than GL -5 m.[7]

DEVELOPMENT OF EARTHQUAKE ACCELERATION DATABASE

Selection of earthquake records

The triggering level of the recording system is comparatively low, and many of the recorded earthquakes are small and give insignificant information. The earthquake records for creation of the observation tower database are selected according to the same criteria as those for the Chiba array database[7], since in further research common usage of data is intended.

The largest event included is the Chibaken-Toho-Oki (Kujukuri Coast Boso Peninsula) Earthquake on December 17, 1987 with peak ground acceleration above 300 cm/s^2 at P501 (GL-1m at borehole P5) and peak acceleration at the roof of the tower above 700 cm/s^2.

Creation of the database

The procedure of creating the database is illustrated by a flowchart on Figure 4. The digital magnetic tapes contain voltage data, which are multiplied by the conversion factor for each channel to obtain acceleration data. Similarly to the organization of the Chiba array database, in order to make the records easily utilizable, heading data are assigned to each record[7]. The heading data include event code (IEQK), component code (ICMP), title of the record, the maximum value of the record, sampling interval and the number of time steps. The last six characters of the title contain information about the location of the accelerometer and the orientation of the data, recorded by the channel. e.g. TRM5EW means a record from the accelerometer at the roof level in the center, oriented along the East-West axis. These notations are shown on Figure 2.

Considering the characteristics of the accelerometers, a baseline correction and a high-cut filtering of the raw data are carried out. (Fig. 4.)

The such obtained data are oriented according to the local XY coordinate system, shown on Figure 1. A transformation of all records is necessary, in order to orient them according to a North-South-East-West coordinate system, which is used in the Chiba array database, and also to remove possible error, due to inaccurate installation. The positive directions for the rotated data are fixed in the horizontal plane from North to South and from East to West . The positive vertical direction is preserved to be upwards, like in the local coordinate system. The evaluation of the angles between local coordinate and North-South-East-West coordinate is done by means of the maximum cross-correlation method.[9] The determined rotation angles for each accelerometer are shown in Table 1.

Finally, the absolute starting time and duration of the records are equalized to that of the corresponding records of the Chiba array database, with regard to the future common usage of both databases.

Table 2 and Table 3 present a list and basic information about the largest nine events in the thus created database.

RESULTS OF PROCESSING OF EARTHQUAKE DATA

Figure 5 and 6 show Fourier spectra of acceleration at some points of interest (GL -40 m at borehole P5, the basement, the ground level floor and the fourth floor of the tower) together with the respective accelerograms. The spectra on Figure 5 are evaluated from records of the largest event, included in the database - the Chibaken-Toho-Oki Earthquake (IEQK 8722) and those on Figure 6 - from the second largest event, Southern Boso Peninsula (IEQK 8525) (cf. Table 2,3). The vertical component shows small amplification and almost identical frequency contents within the structure. It can be seen that the horizontal motions of the basement and the ground level floor are very similar between themselves and noticeably different from the motion of the fourth floor. The frequency, at which highest amplification of the horizontal motion at the top occurs, is lower in the case of the larger event.

The displacements at the measuring points are determined by double integration of the acceleration data. The multidirectional motion, to which the structure was subject by the propagation of the seismic waves is visualized on

Figure 7. The displacement orbits of the measuring points at the basement and the ground level floor have similar shapes and range as that of the surrounding soil (GL -1 m in borehole P5). The ones at the top of the structure have more complex shapes and a considerably larger range. The displacement diagrams, plotted at fixed time moments (Fig.8) are a quantitative representation of the above considerations. The difference in the directions of the displacements gives an idea about the complex variation in time of the three-dimensional displacement line of the structure. Generally, the basement and the ground level floor have small relative displacements, due to the considerable stiffness of the basement walls, while the upper floors experience larger motions, as the stiffness of the upper walls is smaller. It should be pointed out, however, that this effect is apparently dependent on the seismic load. Regarding the smaller IEQK 8525 event, it can be seen, that the range of relative displacements between the fourth floor and the roof is bigger than that of the basement and the ground level floor, but for the larger IEQK 8722 event those ranges are similar. This can be explained with decreasing of the soil support with increase of the amplitude of the exerted dynamic force.

Figure 9 presents perspective plots of the vertical displacements of the basement floor slab at fixed time moments. The time moments are chosen such, that the difference between the displacements of two oppositely located points is the biggest. As the basement floor slab is very rigid, there is almost no bending, but a noticeable rocking effect is observed, in accordance with the results of previous research[6].

The plots of the coherence and Fourier spectrum ratios between the the two borehole acceleration records (Gl -40 m and GL -1m) indicate a soil amplification at a considerable frequency range[8] (Fig 10,11,12). The observed predominant frequencies of the horizontal motion of the surface soil are about 2.3, 5.5 and 9.0 Hz, showing good coincidence with the values, obtained by one-dimensional shear-wave propagation theory[6]. The Fourier amplitudes of the basement and ground level floor accelerations are amplified at these same frequencies, which is in agreement with the observed similarity of the displacements at these locations. The amplification ratio at the higher frequencies is gradually diminishing within the structure from bottom to top, but only at the fourth floor the coherence with P540 and the Fourier spectrum ratio drop at all frequencies above 6 Hz. This signifies that with respect to the horizontal motions, exclusively the part of the structure above the ground level has a

filtering effect to the high frequency components (Fig. 10 (a),(b),(c), (d); 11(a),(b),(c), (d)). The similarity of the frequency characteristics of motions of the basement and the surrounding soil is confirmed by the small values and the small variations of their Fourier spectrum ratio on Figures 11 (e) and 12 (e).
The crests at 2.5 - 3.0 Hz, observed in the Fourier spectrum ratio between P540 and T4FM (Fig. 10 (d) ; 11(d)), most probably represent the effect of the rocking on the horizontal displacement. Namely, the stronger rocking (IEQK 8722) causes a shift of the natural frequency.

Filtering of high frequency components, however, can not be noticed for the vertical motion, whose natural frequency is about 7.5 Hz[6]. At the same time there is virtually no amplification of the UD-component within the structure. Comparing the Fourier spectrum ratios between P540 and the different levels of the structure, it can be seen, that the at the fourth floor the maximum value is only a little higher than those at the basement and the ground level floor (Fig. 12 (b), (c) ,(d)), which is probably caused by the rocking.

ANALYSIS OF DATA FROM MICROTREMOR EXPERIMENTS

A series of experiments with microtremor equipment are conducted in order to study the behavior of the soil - structure system at normal everyday conditions when the vibrations, to which it is subject have very small amplitudes. The observations are carried out using three velocity-type sensors. Removing the noise from the records is done by means of a cosine-type band-pass filter (from 1 to 10 Hz). In order to eliminate the possible effect of unfiltered noise, the data from each recording are divided to five equal parts and the Fourier spectrum of each part is calculated. The such evaluated spectra of data recorded on the fourth floor of the tower are plotted together with the Fourier spectra of velocity of two earthquakes (IEQK=8722 and IEQK= 8525) on Figure 13. It can be seen that the spectra of the different parts of the microtremor record have almost one and the same form. Comparing them with the earthquake spectra suggests that depending on the amplitude of the external excitation, the behavior of the soil-structure system significantly changes. There is a marked shift of the natural frequency from about 4 Hz for the microtremor experiment through 3.5 Hz for a moderate earthquake (IEQK 8525) to 2.5 Hz for the considerably large Chibaken-Toho-Oki Earthquake (IEQK 8722). Figure 14

(coherence and Fourier spectrum ratio between the surface soil and basement records from IEQK 8722 IEQK 8525 and microtremor observations) shows that the coherence drops at 6 Hz in the case of vibrations with small amplitudes while incase of earthquake motions it remains relatively high up to 7 Hz. This suggests that during earthquakes the structure experiences sway and rocking due to the yielding of the surrounding soil under the large amplitude of the exerted force.

CONCLUSIONS

Creating a structure response database of real earthquake records is an useful tool for obtaining of actual characteristics of a dynamic system and investigation of soil-structure interaction. In this particular case, the availability of the Chiba array immediately close to the tower provides the possibility for obtaining highly reliable results, due to the common ground conditions.

As a result of processing of the earthquake records it is found that the characteristics of the motion of the underground part of the tower up to the ground level are similar to those of the surrounding soil, rather than to those of the upper part of the structure. The typical for concrete buildings filtering of the high frequency components is clearly observed only in the higher floors. As the basement floor slab is very rigid, it experiences insignificantly small bending, but a considerable rocking effect is observed. There is no filtering of the high frequency components of the vertical motion, but the vertical component is virtually not amplified within the structure. There is a good agreement between the theoretically evaluated parameters of the soil-structure system and those, obtained by processing of the earthquake records.

Comparison with results from processing of microtremor data shows that with the increasing of the amplitude of the dynamic excitation the natural frequency of the horizontal vibrations of the structure decreases. This is a consequence of the finite stiffness of the supporting soil which yields to a large load and allows the sway and rocking of the structure.

REFERENCES

1. Y. Hangai, F. Tatsuoka and N. Sato, "Observation of Soil - Structure Interaction of Towered Structure.", Seisan - Kenkyu, 35(9), 35-38(1983) (in Japanese).
2. Y. Hangai, T. Tanami and T. Yamagami, "Response Observation of Reinforced Concrete Tower.", Seisan - Kenkyu, 36(9), 24-28(1984) (in Japanese).

3. K. Takanashi, N. Sato and K. Ohi , "Data Acquisition System and Data Processing System" , Seisan - Kenkyu, 35(9), 18-21(1983) (in Japanese).
4. Y. Hangai, T. Tanami and T. Yamagami, "Response Observations of a Reinforced Concrete Tower" Bulletin of Earthquake Resistant Structure Research Center, 18, 49-60 (1985).
5. T. Yamagami and Y. Hangai, "Observations of Dynamic Soil-Structure Interaction of Reinforced Concrete Tower", Bulletin of Earthquake Resistant Structure research Center, 19, 37-45 (1986)
6 T. Yamagami, "Observations of Dynamic Soil-Structure Interaction of Reinforced Concrete Tower", A Dissertation submitted in Partial Fulfillment of the Requirements for the Degree of Doctor of Engineering,1990.
7. T. Katayama, F. Yamazaki, S. Nagata, L. Lu and T. Turker, "A Strong Motion Database for the Chiba Seismometer Array and its Engineering Analysis.", Earthquake Engineering and Structural Dynamics, 19, 1089-1106(1990).
8. L. Lu, F. Yamazaki and T. Katayama, "Soil Amplification Based on Seismometer Array and Microtremor Observations in Chiba, Japan", Earthquake Engineering and Structural Dynamics, 21, 95-108(1992).
9. F. Yamazaki, L. Lu and T. Katayama, "Orientation Error Estimation of Buried Seismographs in Array Observation", Earthquake Engineering and Structural Dynamics, 21, 679-694(1992).

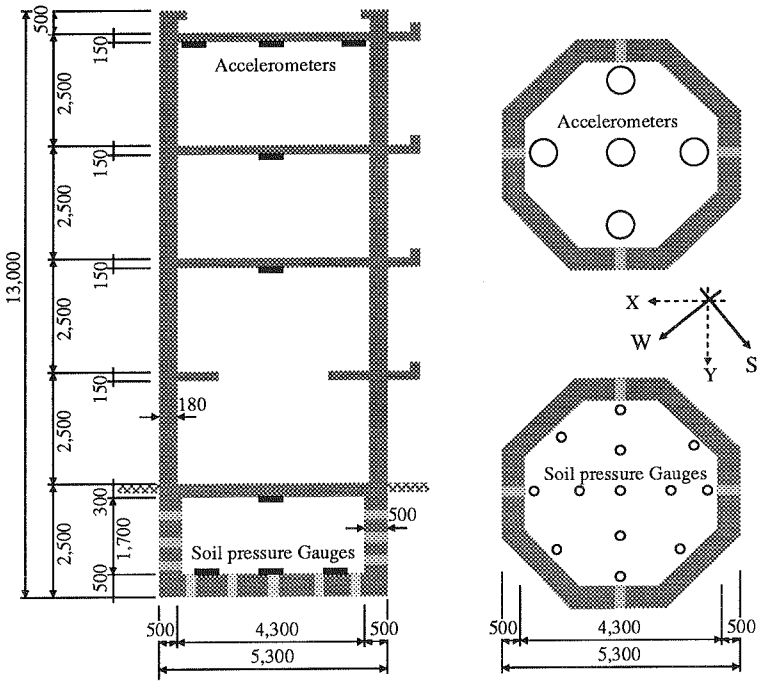

Fig.1. Plan and vertical cross-section of the tower

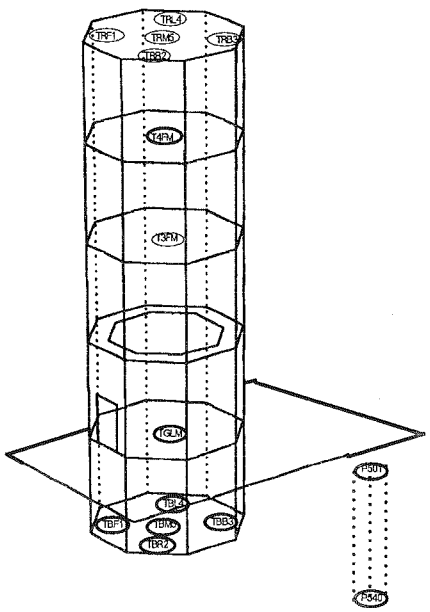

Fig.2. Locations of the accelerometers

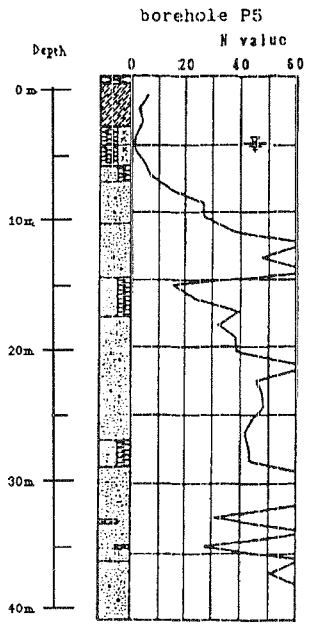

Fig.3. Soil profile at borehole P5

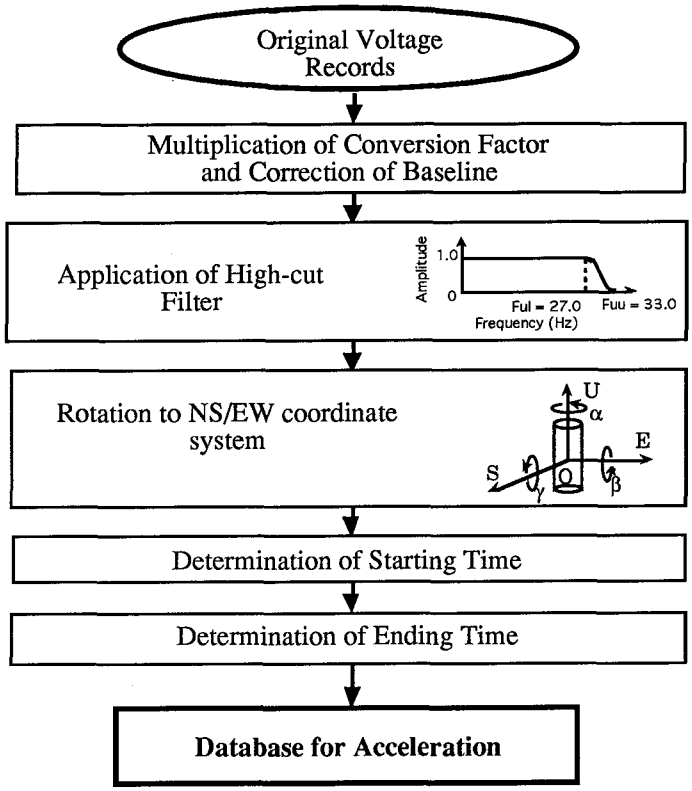

Fig. 4. Procedure for creating the database.

Table 1. Rotation angles with respect to EW-NS coordinate system.

Accelero-meters	Rotation Angles		
	α (deg)	β (deg)	γ (deg)
TRF1	-34.5	-0.3	3.5
TRL4	-33.2	-6.2	7.6
TRB3	-36.4	-6.4	1.0
TRR2	-34.3	-1.7	-1.6
TRM5	-33.5	-2.9	1.7
T4FM	-35.0	-2.9	2.7
T3FM	-39.4	1.2	0.8
TGLM	-33.5	0.3	-0.6
TBF1	-33.9	5.9	0.2
TBL4	-36.0	-1.5	3.7
TBB3	-35.7	-1.2	-3.0
TBR2	-33.0	7.4	-7.5
TBM5	-34.9	1.9	-1.3
P501	- 2.0	2.8	2.4
P540	12.9	0.4	0.1

Table.2. Earthquake Events in The Observation Tower Database

Nº	IEQK	Origin Time by JMA		Epicenter		Focal Depth (km)	JMA Magn	Location of Epicenter
		Date	h/min/s	Lat.(N)	Long(E)			
1	8525	85.11.06	00:30:50	35°21.3'	140°14.4'	63	5.0	Southern Boso Pen.
2	8717	87.06.30	18:17:07	36°11.0'	140°5.3'	57	4.9	SW Ibaraki Pref.
3	8722	87.12.17	11:08:16	35°22.3'	140°29.8'	58	6.7	Kujukuri Coast Boso Pen.
4	8723	87.12.17	11:15:11	35°21.7'	140°30.7'	52	4.6	Kujukuri Coast Boso Pen.
5	8726	87.12.17	15:29:56	35°19.5'	140°33.5'	42	4.0	Kujukuri Coast Boso Pen.
6	8802	88.01.05	10:09:02	35°24.7'	140°26.0'	42	4.2	Kujukuri Coast Boso Pen.
7	8806	88.01.16	20:42:11	35°23.2'	140°24.8'	48	5.2	Kujukuri Coast Boso Pen.
8	8808	88.01.18	19:37:14	35°33.2'	139°56.6'	32	4.1	Tokyo Pref.
9	8816	88.03.18	05:34:29	35°39.7'	139°38.8'	96	6.0	Tokyo Pref.

Table.3. Basic Information on the Earthquake Records

Nº	IEQK	Trigger Time at P540		Focal Depth (km)	JMA Magn	Azimuth (deg)	Epicentral Distance (km)	T_D/T_R (s)	Max Acceleration at P501 (gal)			Max Acceleration at TRM5 (gal)		
		Date	h/min/s						EW	NS	UD	EW	NS	UD
1	8525	85.11.06	00:31:00	63	5.0	158.2	32	35/80	80.0	67.5	29.5	140.6	183.2	41.2
2	8717	87.06.30	18:17:21	57	4.9	358.2	62	43/68	15.7	24.0	12.4	34.6	46.8	15.8
3	8722	87.12.17	11:08:27	58	6.7	128.1	45	39/282	218.6	393.3	120.3	577.9	703.0	159.6
4	8723	87.12.17	11:15:14	52	4.6	128.2	46	51/64	22.9	26.8	11.3	23.4	45.7	21.0
5	8726	87.12.17	15:30:07	42	4.0	128.8	52	24/39	24.0	34.1	18.7	11.4	41.5	20.0
6	8802	88.01.05	10:09:17	42	4.2	128.3	37	17/39	32.2	47.7	10.6	18.6	67.3	15.6
7	8806	88.01.16	20:42:20	48	5.2	133.3	38	37/81	51.4	96.0	19.6	82.9	148.0	27.3
8	8808	88.01.18	19:37:24	32	4.1	243.6	17	19/34	26.6	28.7	7.2	28.3	14.1	9.0
9	8816	88.03.18	05:34:45	96	6.0	276.3	42	59/138	58.0	42.0	42.3	115.4	163.5	37.0

T_D - Duration of Database Record ; T_R - Duration of Original Record ; Azimuth - clockwize from North

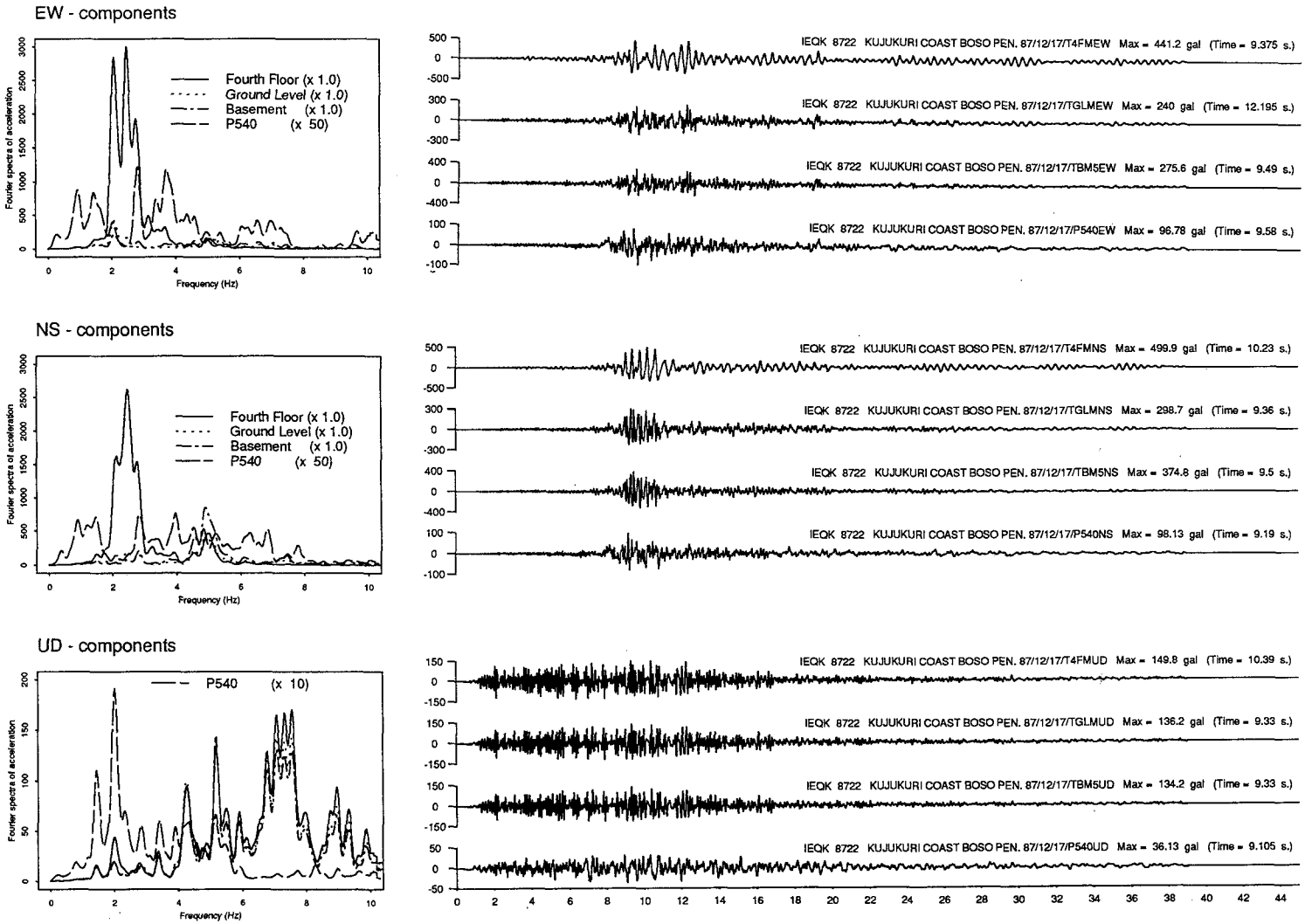

Fig. 5 Fourier spectra and wave forms (IEQK 8722)

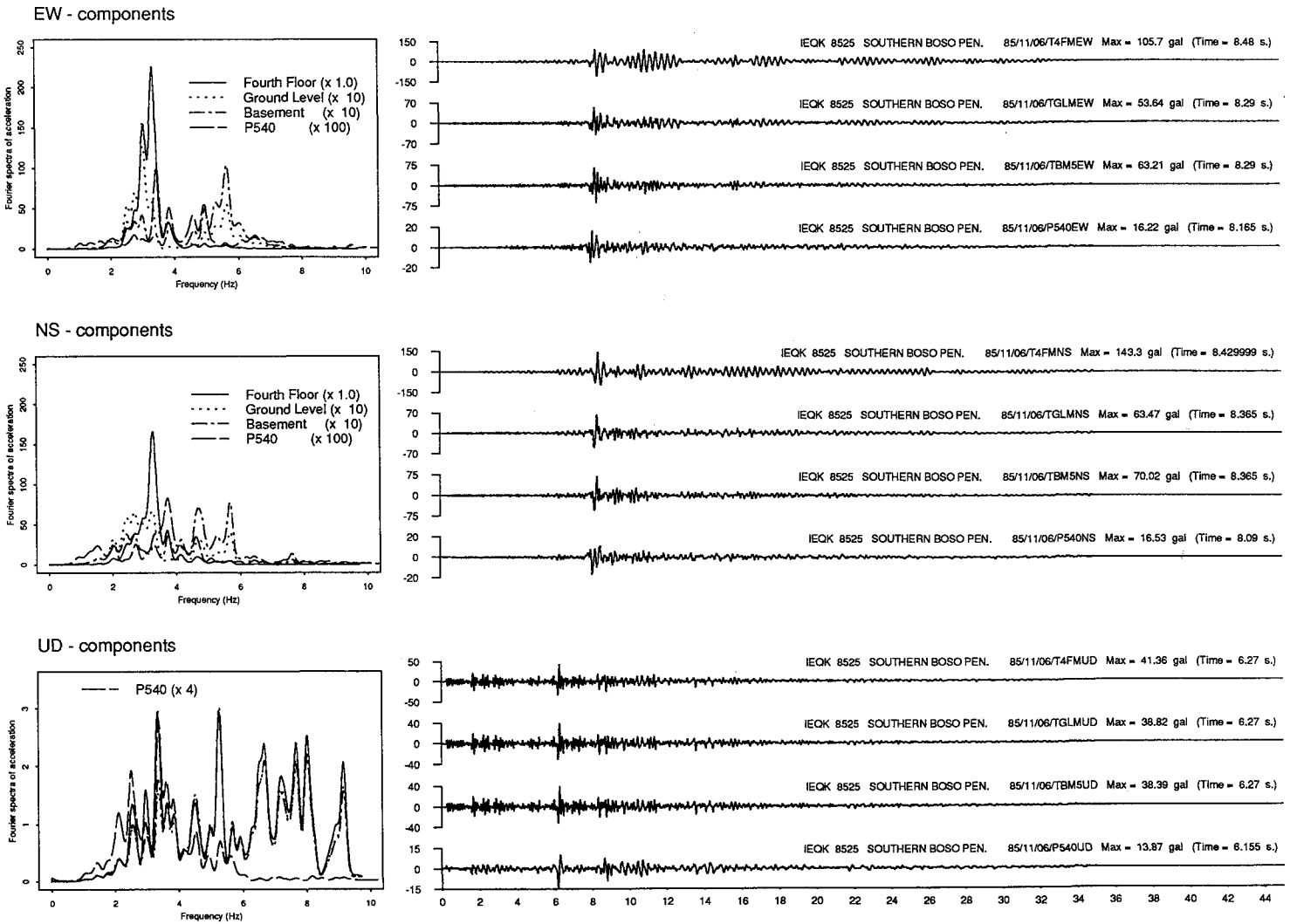

Fig. 6 Fourier spectra and wave forms (IEQK 8525)

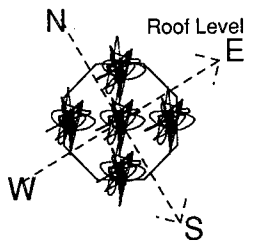

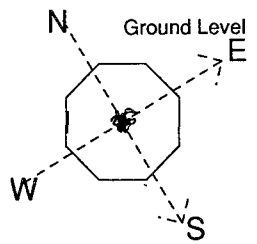

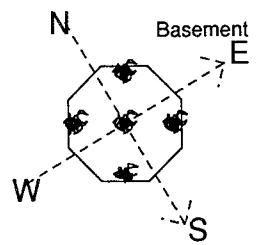

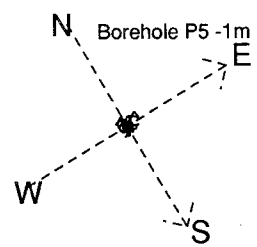

Kujukuri Coast Boso Pen. 87/12/17
IEQK 8722, time : 8 to 13s

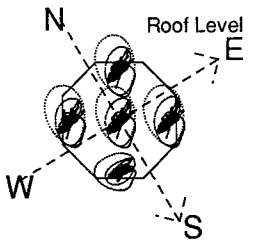

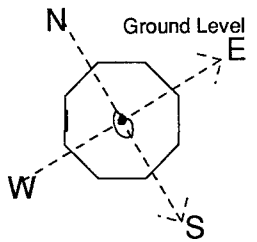

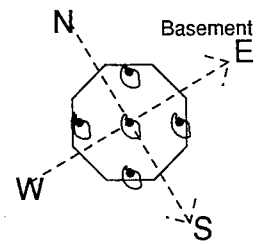

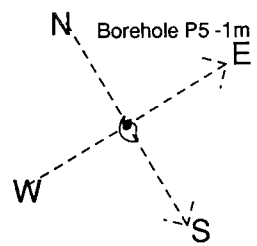

Southern Boso Pen. 85/11/06
IEQK 8525, time : 8 to 13s

Fig.7. Displacement orbit graphs

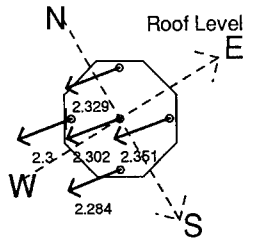

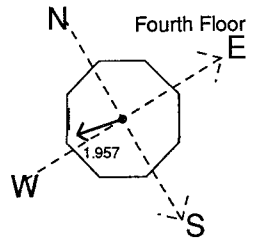

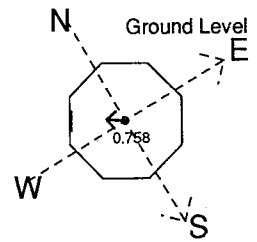

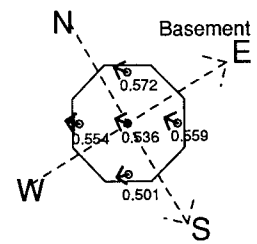

Kujukuri Coast Boso Pen. 87/12/17
IEQK 8722 , time 12.24 s

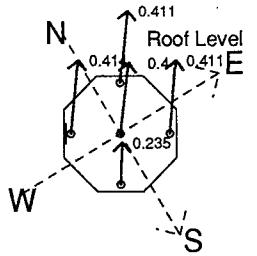

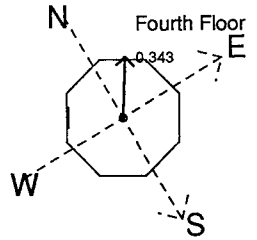

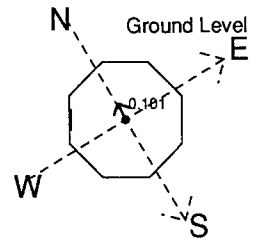

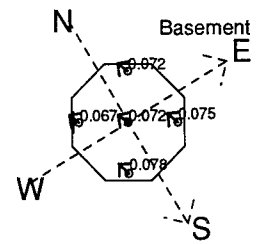

Southern Boso Pen. 85/11/06
IEQK 8525 , time 8.47s

Fig.8. Diagrams of displacements (cm)

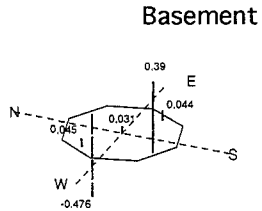

Kujukuri Coast Boso Pen. 87/12/17
IEQK 8722, time : 10.67 s

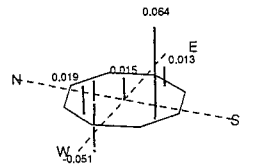

Southern Boso Pen. 85/11/06
IEQK 8525, time : 8.46 s

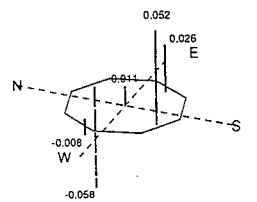

Kujukuri Coast Boso Pen. 88/01/16
IEQK 8806, time 7.485 s

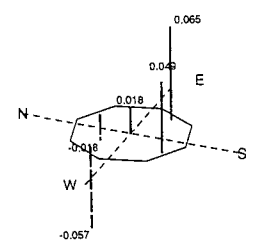

Tokyo Prefecture 88/03/18
IEQK 8816 , time 13.455 s

Fig.9. Vertical Displacements (cm)

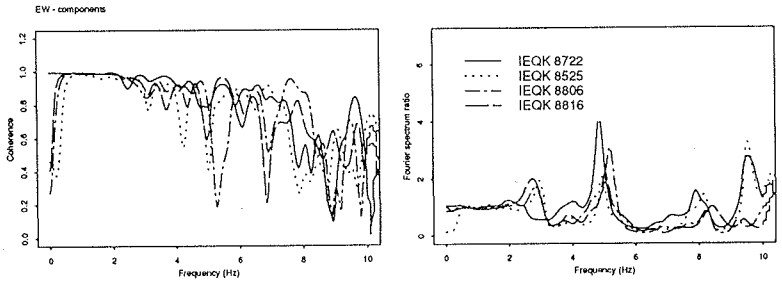

(e) Coherence function and Fourier spectrum ratio between P501 and TBM5

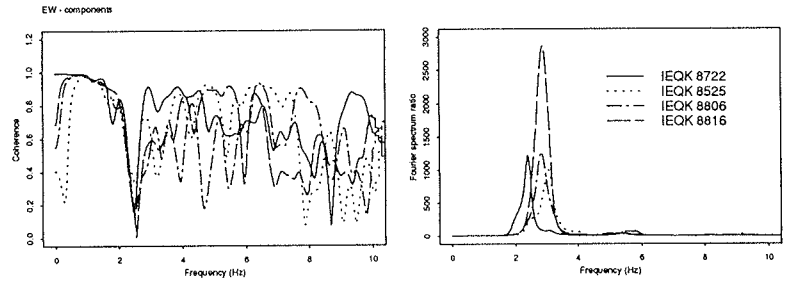

(d) Coherence function and Fourier spectrum ratio between P540 and T4FM

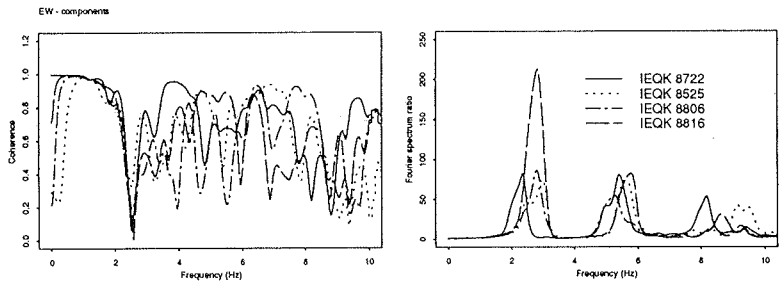

(c) Coherence function and Fourier spectrum ratio between P540 and TGLM

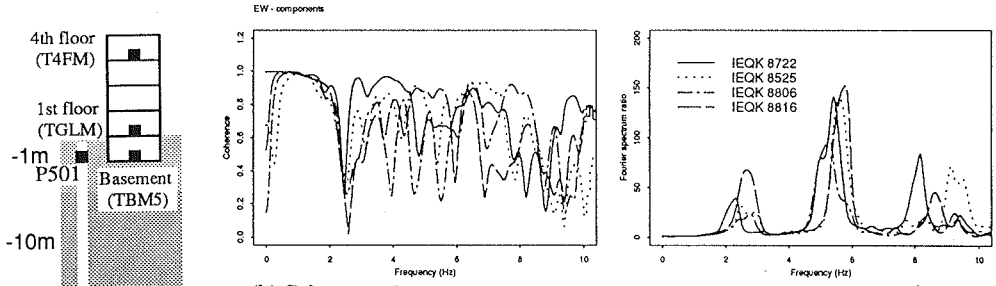

(b) Coherence function and Fourier spectrum ratio between P540 and TBM5

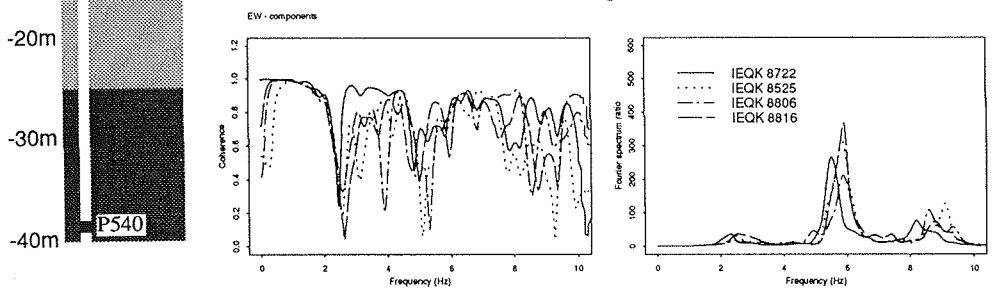

(a) Coherence function and Fourier spectrum ratio between P540 and P501

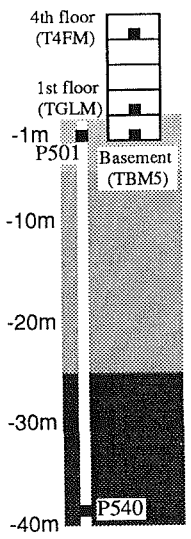

Fig. 10 Comparison of coherence functions and Fourier spectrum ratios (EW component)

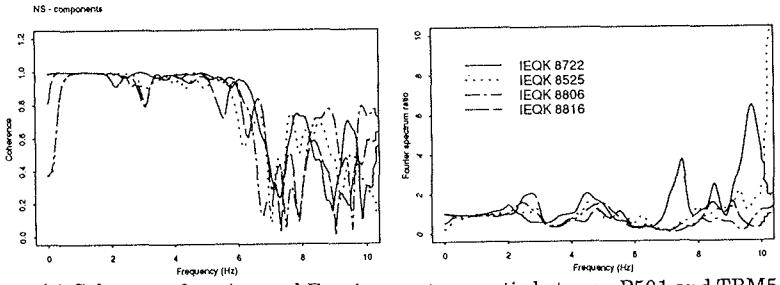

(e) Coherence function and Fourier spectrum ratio between P501 and TBM5

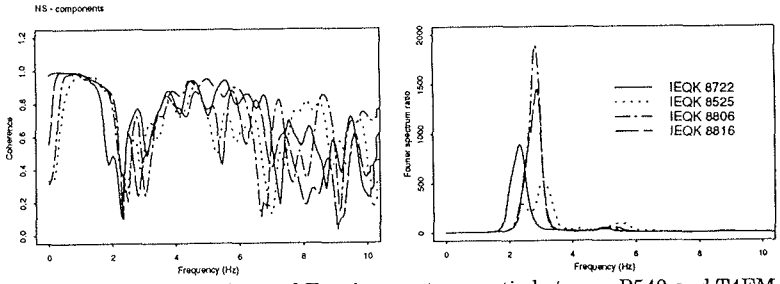

(d) Coherence function and Fourier spectrum ratio between P540 and T4FM

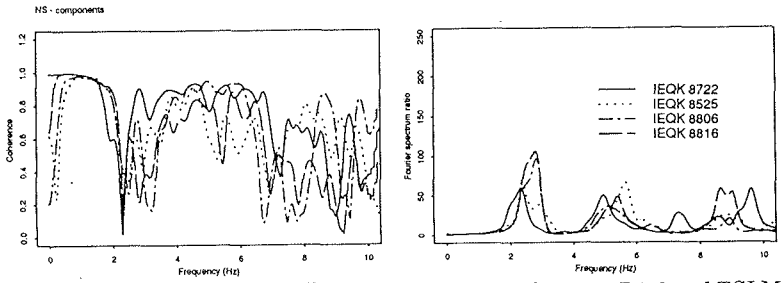

(c) Coherence function and Fourier spectrum ratio between P540 and TGLM

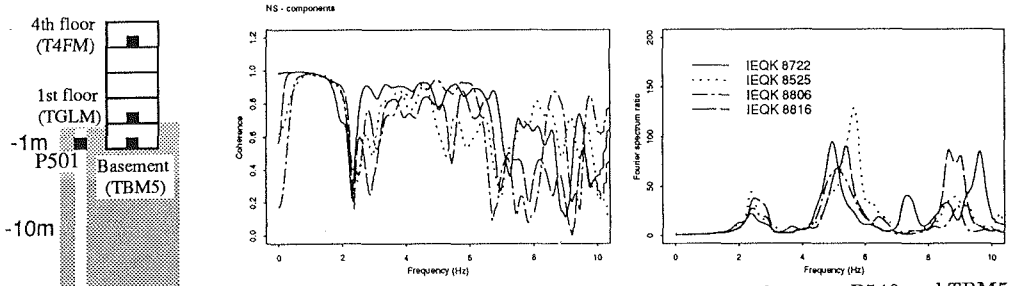

(b) Coherence function and Fourier spectrum ratio between P540 and TBM5

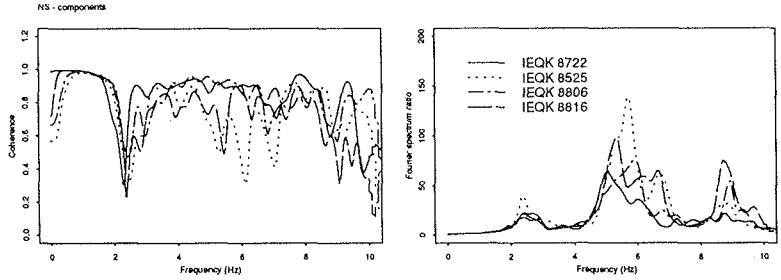

(a) Coherence function and Fourier spectrum ratio between P540 and P501

Fig. 11 Comparison of coherence functions and Fourier spectrum ratios (NS component)

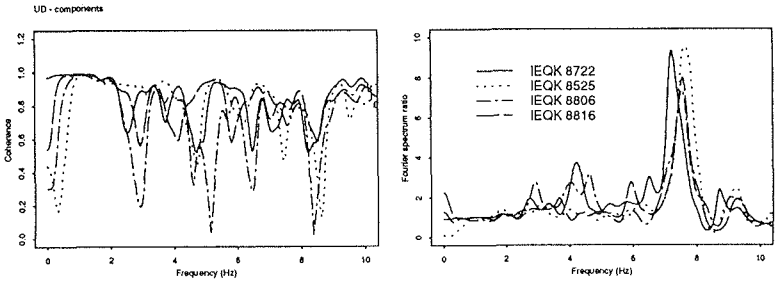

(e) Coherence function and Fourier spectrum ratio between P501 and TBM5

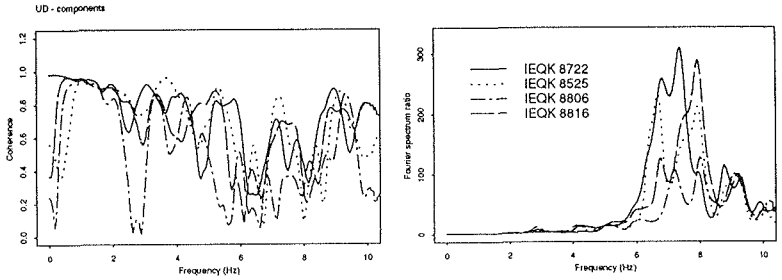

(d) Coherence function and Fourier spectrum ratio between P540 and T4FM

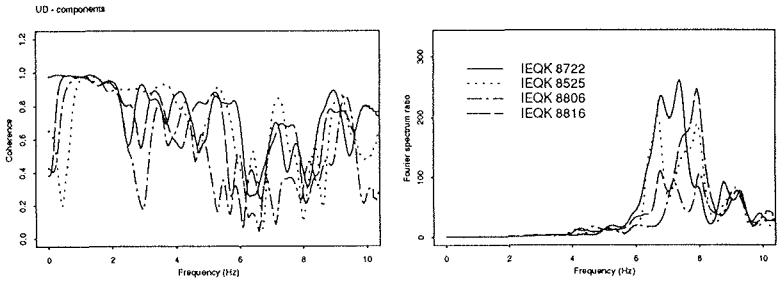

(c) Coherence function and Fourier spectrum ratio between P540 and TGLM

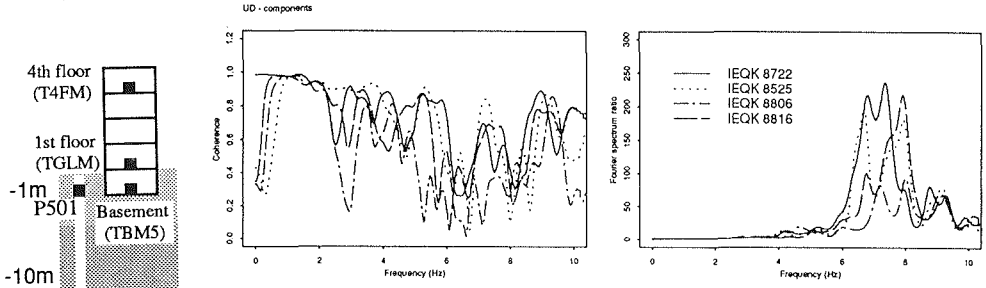

(b) Coherence function and Fourier spectrum ratio between P540 and TBM5

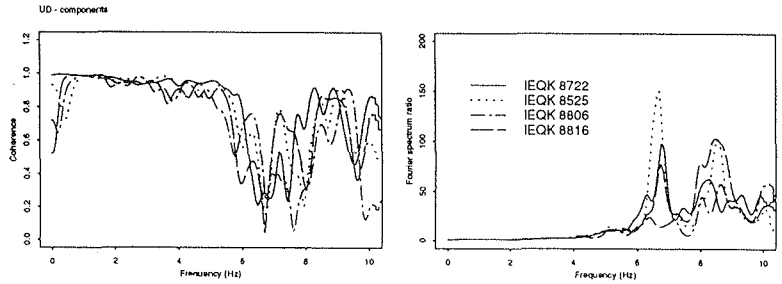

(a) Coherence function and Fourier spectrum ratio between P540 and P501

Fig. 12 Comparison of coherence functions and Fourier spectrum ratios (UD component)

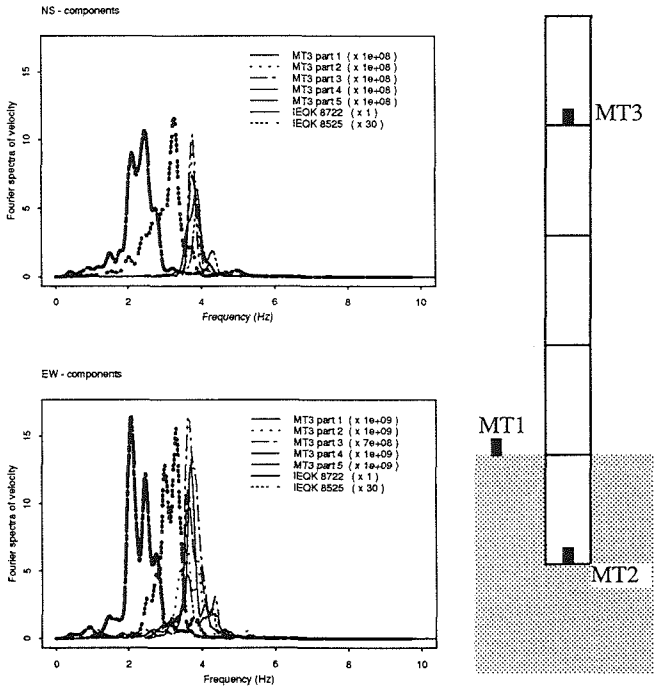

Fig. 13 Comparison of Fourier spectra of earthquake response and microtremor

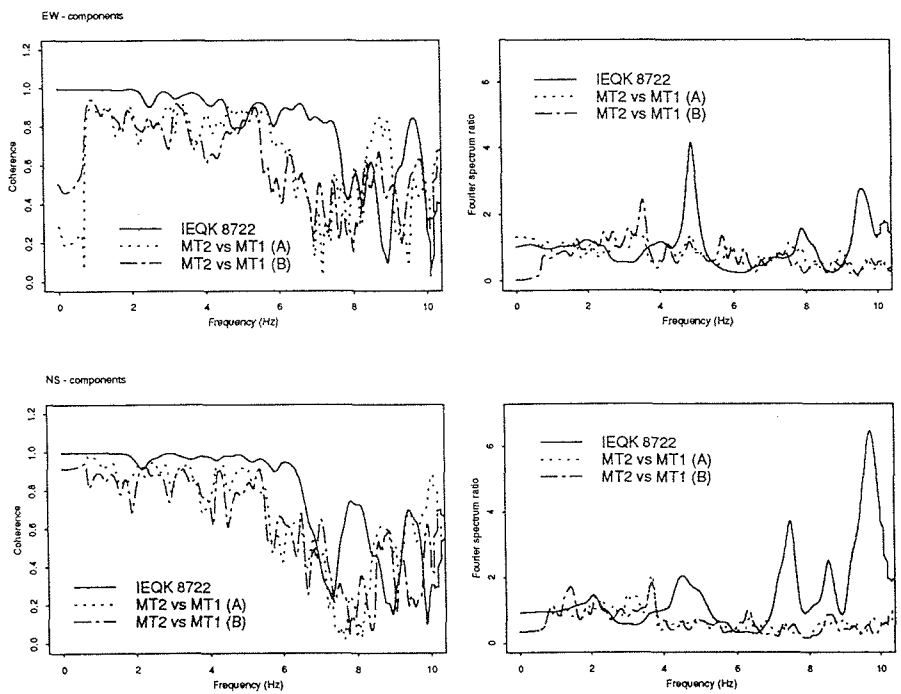

Fig. 14 Comparison of coherence functions and spectrum ratios of earthquake response and microtremor